



LAWRENCE
LIVERMORE
NATIONAL
LABORATORY

On the Potential for Vacancy Annihilation as a Mechanism for Conditioning in Pu-1.9 at.% Ga

J. R. Jeffries, K. J. M. Blobaum, A. J. Schwartz

March 31, 2009

Acta Materialia

Disclaimer

This document was prepared as an account of work sponsored by an agency of the United States government. Neither the United States government nor Lawrence Livermore National Security, LLC, nor any of their employees makes any warranty, expressed or implied, or assumes any legal liability or responsibility for the accuracy, completeness, or usefulness of any information, apparatus, product, or process disclosed, or represents that its use would not infringe privately owned rights. Reference herein to any specific commercial product, process, or service by trade name, trademark, manufacturer, or otherwise does not necessarily constitute or imply its endorsement, recommendation, or favoring by the United States government or Lawrence Livermore National Security, LLC. The views and opinions of authors expressed herein do not necessarily state or reflect those of the United States government or Lawrence Livermore National Security, LLC, and shall not be used for advertising or product endorsement purposes.

On the Potential for Vacancy Annihilation as a Mechanism for Conditioning in Pu-1.9 at.% Ga

J. R. Jeffries, K. J. M. Blobaum, and A. J. Schwartz
Lawrence Livermore National Laboratory, Livermore, CA 94550, USA
(Dated: March 31, 2009)

The $\delta \rightarrow \alpha'$ martensitic transformation in Pu-1.9 at.% Ga occurs when the alloy is cooled below about -100 °C. This transformation exhibits anomalous behavior, where the isothermal transformation proceeds atypically with double-C kinetics. Recent work has revealed that an ambient-temperature isothermal hold (referred to as conditioning) prior to the transformation has different effects depending on whether transformation proceeds in the upper- or lower-C of the double-C: the amount of transformation is increased with conditioning in the upper-C, while the transformation in the lower-C seems to be engendered by conditioning. The mechanism by which conditioning affects the low-temperature $\delta \rightarrow \alpha'$ transformation is thus of great importance to understanding the transformation itself as well as the general circumstances that can affect a martensitic phase transformation. Using differential scanning calorimetry measurements, vacancy annihilation as a mechanism for the conditioning effect has been examined. While there are some characteristics of the conditioning effect that are reminiscent of vacancy annihilation, the results of these experiments suggest that vacancy annihilation is not a likely candidate description for the conditioning effect.

PACS numbers: 81.40.Gh, 81.30.Kf, 61.72.jd

I. INTRODUCTION

Martensitic transformations are diffusionless structural transitions that yield a product phase with a specific orientation relationship to the parent phase.¹ These transformations occur through a rapid, displacive, shear-like motion of atoms, and are driven by a combination of thermodynamic and kinetic considerations, meaning that state variables (*e.g.*, temperature, pressure, magnetic field, etc.), chemical composition, and the time rate of change of those quantities can have dramatic implications on a martensitic transformation. Martensitic transformations can be manipulated with magnetic fields,² their formation can be a function of cooling rate,³ and the product phase morphology can be dependent on the temperature history.⁴ Despite the fact that there are many variables affecting a martensitic transformation, these transformations are involved in technological applications ranging from shape memory alloys to structural materials.⁵

Martensitic transformations can be loosely divided into two classes: athermal and isothermal.⁶ The eponymous transformation in Fe-C steel belongs to the former category (athermal), where the amount of transformation is dependent only on temperature. The second class (isothermal), to which Pu-Ga alloys belong,⁷ exhibit a dependence on both time and temperature. A time-temperature-transformation (TTT) diagram—where the amounts of transformation are plotted as contours in a temperature-time plane, typically with time as the abscissa—is often employed to represent the temperature and time evolution of a phase transformation. On a TTT diagram, the beginning of an athermal martensitic transformation is represented by a horizontal line (parallel to the time axis) at the martensite start temperature (M_s), while the completion of that athermal transformation is

indicated by another horizontal line at a lower martensite finish temperature (M_f). On the contrary, an isothermal martensitic transformation appears as a C-shaped curve in a TTT diagram, where the C-shape derives from competing energy scales affecting the formation of the martensitic product. Because there are many time and temperature coordinates that yield a given amount of transformation, it is difficult to uniquely define an M_s or M_f temperature for an isothermal martensite, but the nose temperature, the temperature at which transformation occurs in a minimal amount of time, can be used as a benchmark temperature for a transformation.

Because of their critical role in advanced materials, it is imperative to understand how martensitic transformations can be impeded or promoted by processing, aging, thermal history, and other mechanisms. Pu-Ga alloys provide a platform to investigate several important factors as they may relate to the formation of the martensitic product including self-irradiation from the nuclear decay of Pu atoms, the proximity of nearly degenerate structural phases within a free energy landscape, phase-dependent Ga immiscibility, lattice defects, and strains.^{8–10}

A Pu-1.9 at.% Ga alloy exhibits an isothermal martensitic transformation where the parent face-centered-cubic δ phase—which is metastable for $T \lesssim 200$ °C—incompletely transforms into the product α' phase below a temperature of approximately -100 °C.¹¹ The α' phase forms with the same monoclinic symmetry as the unalloyed α -Pu structure, but with expanded lattice parameters due to trapped Ga solute (the “prime” is conventionally used to represent this Ga-containing, expanded structure).⁸ Although only partial, this transformation is commonly denoted as the $\delta \rightarrow \alpha'$ transformation, and typically results in a fractional amount of α' phase less than 25%.¹² This low fractional amount of transforma-

tion is thought to be a result of the large volume collapse (about 18%) coinciding with the transformation, which generates large elastic and plastic strain fields that ultimately arrest the transformation.^{13,14} The isothermal character of the $\delta \rightarrow \alpha'$ transformation is peculiar in that the transformation evinces a double-C when plotted on a TTT diagram; that is, there are two nose temperatures that define local minima in the amount of time required to form a certain volume fraction of α' phase.⁷ The root causes of the double-C in Pu-1.9 at.% Ga have remained shrouded for over three decades, but recent microstructural characterization suggests that a “conditioning” treatment dramatically affects the $\delta \rightarrow \alpha'$ transformation: transformation in the upper-C is enhanced with conditioning, while transformation in the lower-C is enabled by conditioning.¹⁵

Conditioning a Pu-1.9 at.% Ga specimen is achieved by isothermally holding the sample at a temperature between $-50\text{ }^\circ\text{C} \lesssim T_{cond} \lesssim 200\text{ }^\circ\text{C}$ for several hours.¹⁶ If a previously transformed sample is annealed (held at $375\text{ }^\circ\text{C}$ for several hours) and then conditioned, then the amount of α' phase resulting from the $\delta \rightarrow \alpha'$ transformation will be much greater than if the sample were not conditioned. Conditioning exhibits a maximum effectiveness at increasing the amount of $\delta \rightarrow \alpha'$ transformation for hold times of eight or more hours at the optimal conditioning temperature of $25\text{ }^\circ\text{C}$; hold times in excess of approximately 8 hours do not produce an increase in the amount of martensitic transformation. After optimal conditioning, the amount of α' phase formed at low temperature can be increased by a factor of two or more.¹⁵ The amount of transformation is reduced from maximal as the conditioning temperature deviates from the optimal conditioning temperature or if the conditioning time is reduced.¹⁶

At low homologous temperatures (the homologous temperature is the ratio of the absolute temperature to that of the melting point T_M), atomic diffusion is exponentially suppressed, and conventional metals are generally regarded as unchanging. The conditioning effect in Pu-1.9 at.% Ga is quite surprising as it occurs at a relatively low homologous temperature, yet the dramatic change in the amount of α' phase formed during the low-temperature $\delta \rightarrow \alpha'$ transformation suggests that a Pu-1.9 at.% Ga alloy is anything but unchanging on the relatively short time scales of conditioning. The mechanisms by which conditioning promotes the $\delta \rightarrow \alpha'$ transformation in Pu-Ga alloys are not currently understood, but these mechanisms are of great importance to the phase stability of the Pu-Ga system, but also to our more general appreciation of external factors that can alter a martensitic phase transformation.

While the conditioning effect in Pu-1.9 at.% Ga alloys occurs at a relatively low homologous temperature ($T_{cond} \approx 0.3T_M$) where diffusion and strain relaxation are suppressed, these alloys do not comprise exclusively an exhaustive group of materials where isothermal treatments at low homologous temperature affect marten-

sitic transformations. The Au-49.5 at.% Cd binary alloy, for which T_M is comparable to Pu-1.9 at.% Ga, has been shown to exhibit an athermal martensitic transformation from the parent β phase (Cs-Cl structure) to the non-centrosymmetric ζ' phase (trigonal), which forms via a rhombahedral distortion of the β phase.^{17,18} When a specimen of Au-49.5 at.% Cd is quenched from high temperature, M_S for the $\beta \rightarrow \zeta'$ transformation decreases by nearly $20\text{ }^\circ\text{C}$ compared to a slow-cooled specimen.¹⁹ When the previously transformed sample is reverted to the parent phase and then isothermally held near room temperature, M_S increases upon subsequent cooling and transformation. As the isothermal hold time is increased, M_S converges toward the value of a slow-cooled specimen. This room-temperature “aging” behavior has been attributed to the annealing of excess vacancies trapped during the quench from high temperature;²⁰ the quenched-in vacancies effectively stabilize the β phase, and isothermally annealing the vacancies recovers the equilibrium behavior of the phase transformation.¹⁹ In an opposite manner, quenched-in vacancies have been shown to have a tendency toward stabilizing the martensitic phases of Cu-Al-Mn and Cu-Zn-Al shape memory alloys.^{21,22}

It has been proposed that conditioning is the result of the nucleation of embryos of stable phases. Upon cooling, these embryos could serve as additional nucleation sites for the $\delta \rightarrow \alpha'$ transformation, thus increasing the amount of transformation. However, like Au-49.5 at.% Cd, it is not inconceivable that the thermal procedures that produce the conditioning effect in Pu-Ga alloys are conducive to vacancy formation and subsequent annihilation. As such, we have experimentally investigated the potential for ascribing the conditioning effect in Pu-1.9 at.% Ga alloys to the time-dependent annihilation of excess quenched-in vacancies. Herein we report a systematic study designed to distinguish a vacancy annihilation scenario as a description of conditioning from that of embryo nucleation.

II. EXPERIMENTAL DETAILS

A 177 mg, 3-mm diameter disc of Pu-1.9 at.% Ga was used for differential scanning calorimetry measurements. The isotopic and chemical compositions of this sample have been reported elsewhere.¹⁵ The sample was loaded into a gold-plated stainless steel pan that was subsequently installed in a Perkin-Elmer Pyris Diamond differential scanning calorimeter (DSC). All isothermal holds and continuous cooling treatments were performed within the instrument.

In order to ensure a reproducible starting point for each individual experiment, the sample was annealed at $375\text{ }^\circ\text{C}$ for 4 hours before any other thermal procedures.²³ From this starting point, the sample was cooled to $0\text{ }^\circ\text{C}$ at $200\text{ }^\circ\text{C}/\text{min}$, the maximum reliable cooling rate that the instrument could achieve over this entire temperature

window, or 50 °C/min. Herein, the term “quench” has been used to indicate cooling, regardless of rate, from the anneal temperature down to the conditioning temperature. This quench was not expected to circumvent the formation of other stable phases, but the terminology has been borrowed in order to denote the potential importance of the process, particularly with respect to vacancy concentration. Once at 0 °C, the sample was conditioned (isothermally held) for various times up to 16 hours. Following this conditioning treatment, the sample was cooled at 20 °C/min to -160 °C (the base temperature of the DSC) to instigate the $\delta \rightarrow \alpha'$ transformation. The sample was then warmed to 375 °C at 20 °C/min to allow for the $\alpha' \rightarrow \delta$ reversion.

A smooth baseline was subtracted from the raw DSC heat flow data to reveal the $\alpha' \rightarrow \delta$ reversion peak. The area under the reversion peak gave the measured heat of reversion, which was determined by numerically integrating the heat flow data.

III. RESULTS

Figure 1 shows a subset of the collected DSC traces (*i.e.*, heat flow versus temperature) for the $\alpha' \rightarrow \delta$ reversion for several conditioning times following a quench at 50 °C/min. For clarity, the heat flow data for additional conditioning times have been excluded from Figure 1: 8, 6, 3, 2.5, 1.5, and 0.5 hours. The DSC traces show a characteristic peak structure associated with the $\alpha' \rightarrow \delta$ reversion, but the height of the peak decreases with decreasing conditioning time. Furthermore, the heat flow data evince an oscillatory structure, previously proposed as a signature of the burst nature of the transformation,²⁴ on the high-temperature side of the reversion, but this structure becomes less pronounced for lower conditioning times. A qualitatively identical behavior is observed when the sample is quenched at 200 °C/min, but the specific time dependence differs. The disparities between the data corresponding to different quench rates are best viewed through the measured heat of reversion.

The reversion peaks represented in Figure 1 can be integrated to obtain the measured heats of reversion, which are displayed in Figure 2 as a function of conditioning time at 0 °C. Figure 2 includes the conditioning-time dependence of the measured heat of reversion for 200-°C/min and 50-°C/min quenches. Both cooling rates show an increase in the measured heat of reversion with increasing conditioning time out to 16 hours. For long conditioning times ($t \gtrsim 3$ hours), the slower quench results in a slightly larger amount of transformation when compared with the faster quench. The opposite is true for short conditioning times ($t \lesssim 3$ hours), where the faster quench results in more transformation than the slower quench. Both cooling rates tend toward zero measured heat with zero conditioning time. Unlike those corresponding to the fast quench, the results for the 50-°C/min curve clearly show an extended period of time

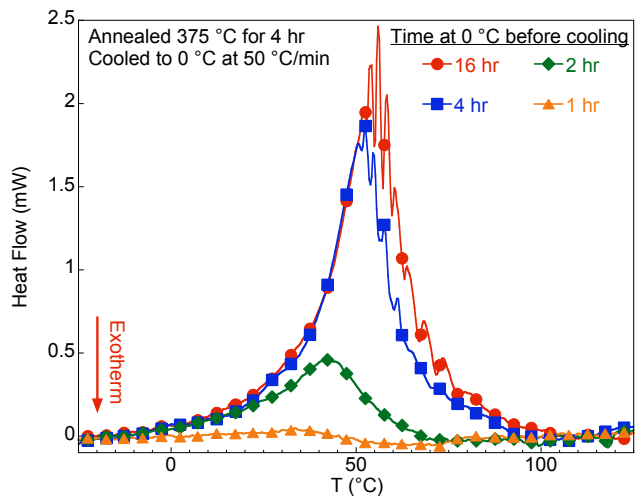


FIG. 1: DSC traces of the heat flow as a function of temperature focusing on the temperature window where the $\alpha' \rightarrow \delta$ reversion occurs. The heat flow is shown for four different conditioning times at 0 °C: 16, 4, 2, and 1 hour(s). An exothermic reaction would evince a negative heat flow, as indicated by the downward, labeled arrow.

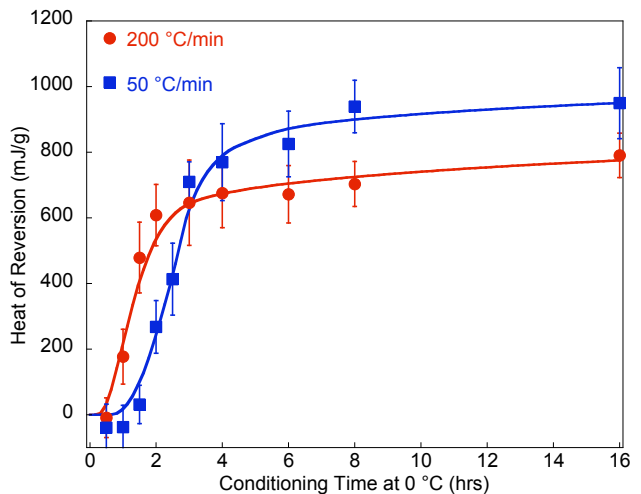


FIG. 2: The measured heat of reversion versus conditioning time at 0 °C for a sample cooled from 375 °C at 200 and 50 °C/min. The solid lines are guides to the eye.

(at low time) where conditioning does not increase the amount of transformation. The implications of these results on the potential for vacancy annihilation as a description of conditioning are discussed below.

IV. DISCUSSION

A. General Behaviors of Vacancy Annihilation with Time and Temperature

If a specimen is held at elevated temperature (*e.g.*, during an anneal), then vacancies will become thermally populated. The equilibrium concentration (c_{eq}) of these thermally populated vacancies at a given temperature is described by:

$$c_{eq}(T) = e^{-H_{vf}/T},$$

where H_{vf} is the vacancy formation energy and T is the temperature, with both quantities specified in Kelvin.²⁵ The temperature dependence of c_{eq} is included later in Figures 4(a) and 5(a).

As a specimen is cooled from a high-temperature anneal, the cooling rate and the vacancy annihilation processes dictate whether the vacancy concentration evolves along (“slow” cooling rates) or deviates from (“fast” cooling rates) the expected equilibrium line. Any deviations from the equilibrium vacancy concentration upon cooling to a final temperature, T_f , would then result in a population of “quenched-in” vacancies greater than the expected equilibrium vacancy concentration at T_f . After the cooling treatment, if the sample containing quenched-in vacancies is isothermally held at T_f , then there exists a driving force for the vacancy concentration to decay to its equilibrium value through the annihilation of these quenched-in vacancies. The processes of quenching excess vacancies into a specimen and the subsequent isothermal decay of those quenched-in vacancies are functions of material-dependent parameters, initial temperatures, final temperatures, and cooling rates.

The vacancy concentration, c , as a function of time and temperature can be assumed to be governed by the following power law rate equation:

$$\dot{c} = -r(c - c_{eq})^n, \quad (1)$$

where \dot{c} is the time rate of change of the vacancy concentration, r is the vacancy annihilation rate, and n is the order at which the annihilation occurs.^{26,27} The vacancy annihilation rate is itself a function of temperature:

$$r(T) = Ae^{-H_m/T},$$

where H_m is the vacancy migration energy barrier and A is a constant encompassing the number of jumps per second each vacancy makes and the average number of jumps required for a vacancy to annihilate.²⁵

Equation 1 can be expressed in integral form as:

$$\int_{c_0}^c \frac{dc}{(c - c_{eq})^n} = -\int_0^t r dt, \quad (2)$$

where c_0 is the starting vacancy concentration at $t = 0$. The general solution of Equation 2 for $n > 1$ is:

$$\frac{1}{[c - c_{eq}]^{n-1}} - \frac{1}{[c_0 - c_{eq}]^{n-1}} = (n-1) \int_0^t r dt, \quad (3)$$

while, for the specific case of $n = 1$, Equation 2 yields a more familiar exponential decay formula:

$$\ln\left(\frac{c - c_{eq}}{c_0 - c_{eq}}\right) = -\int_0^t r dt. \quad (4)$$

Recalling that the vacancy annihilation rate is a function of temperature, the integral of the right hand sides of Equations 2–4 can be defined as:

$$\int_0^t r dt \equiv \mathcal{R},$$

where \mathcal{R} is an implicit function of temperature through r and time through the integration. Equations 3 and 4 can be rearranged to express the excess vacancy concentration (*i.e.*, the vacancy concentration in excess of the expected equilibrium vacancy concentration) in terms of \mathcal{R} :

$$c - c_{eq} = \begin{cases} (c_0 - c_{eq}) e^{-\mathcal{R}} & \text{for } n = 1 \\ \frac{(c_0 - c_{eq})}{[(n-1)(c_0 - c_{eq})^{(n-1)} \mathcal{R} + 1]^{1/(n-1)}} & \text{for } n > 1. \end{cases} \quad (5)$$

Equation 5 thus describes the decay of excess vacancies, where the time and temperature dependences are encompassed in the function \mathcal{R} . The function \mathcal{R} can now be examined for two specific thermal treatments relevant to Pu-Ga: continuous cooling, where \mathcal{R}_c can be reduced to a function of T alone; and an isothermal hold, where \mathcal{R}_{iso} is only a function of t .

For the case of a specimen continuously cooled from a high-temperature anneal at constant cooling rate $\nu = dT/dt$, \mathcal{R} can be expressed as:

$$\mathcal{R}_c(T) = \frac{1}{\nu} \int_{T_0}^{T_f} Ae^{-H_m/T} dT, \quad (6)$$

where T_0 and T_f represent the initial and final temperatures of the cooling treatment. This expression for \mathcal{R}_c can be substituted into Equation 5 to determine the vacancy concentration as a function of temperature upon continuous cooling. Concordant with accepted metallurgical wisdom, a larger cooling rate ν results in a smaller value of \mathcal{R}_c , which results in a larger concentration of excess vacancies that become quenched-in during cooling.

For the case of a specimen isothermally held at a fixed temperature, \mathcal{R} simply becomes a function of time:

$$\begin{aligned}\mathcal{R}_{iso}(t) &= r t \\ &= A e^{-H_m/T} t.\end{aligned}\quad (7)$$

Substituting the expression for \mathcal{R}_{iso} into Equation 5 provides a means to evaluate the time-dependent decay of excess vacancies at a fixed temperature.

The order at which the annihilation of vacancies occurs quantitatively affects the concentration of excess vacancies on cooling as well as during an isothermal hold. The quantitative differences between decay processes of differing order are most readily illustrated by the isothermal decay of excess quenched-in vacancies, which can be seen in Figure 3. While first order and higher order vacancy annihilation both proceed monotonically in time, the latter has a more rapid early-time decay followed by a shallower late-time decay than the former. In addition, the order of the decay process implies specific behavior for the half-life of any excess vacancy concentration.

The half-life occurs at a time, $t_{1/2}$, that satisfies:

$$c(t_{1/2}) - c_{eq} = \frac{1}{2}(c_0 - c_{eq}),$$

which yields from Equation 5 the following solutions for $t_{1/2}$:

$$t_{1/2} = \begin{cases} \frac{\ln 2}{r} & \text{for } n = 1 \\ \frac{2^{(n-1)} - 1}{(n-1)(c_0 - c_{eq})^{(n-1)} r} & \text{for } n > 1. \end{cases}$$

Immediately noticeable is the fact that the half-life of a first order decay process is independent of the initial concentration of excess vacancies ($c_0 - c_{eq}$), while the half-life of any higher order decay processes is dependent on the initial concentration of excess vacancies. Thus, some information about the order of the vacancy annihilation process can be inferred from the evolution (or lack thereof) of the half-life of the excess vacancy concentration as a function of the initial concentration of excess vacancies.

To illustrate the effects of the order n of the decay process on the decay of excess vacancies, Figure 3 shows the time dependence of the relative excess vacancy concentration ($(c(T) - c_{eq}) / (c_0 - c_{eq})$) for first and second order processes and for two different initial excess vacancy concentrations. Figure 3(a) represents decay from a low initial vacancy concentration, while Figure 3(b) represents decay from a higher initial vacancy concentration. The horizontal, dashed line indicates half of the initial excess vacancy concentration. Note that the relative concentration of excess vacancies in first order decay process is independent of initial excess vacancy concentration, with a half-life (downward, blue arrows) defined only by the annihilation rate. The second order process, however, shows a dependence upon the initial concentration of excess vacancies, and the half-life (downward, red arrows) moves to shorter time with increasing initial excess vacancy concentration.

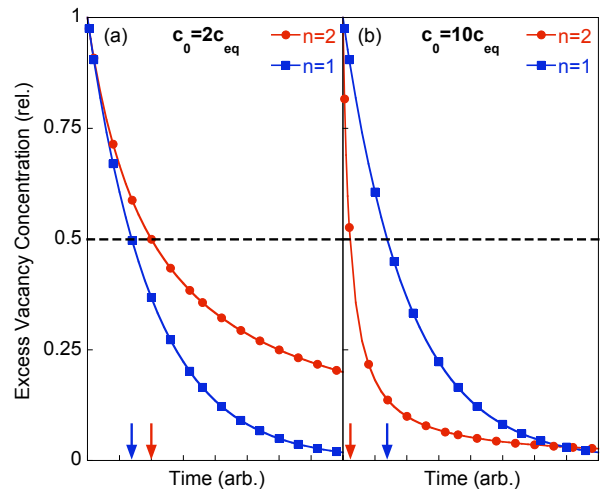


FIG. 3: Relative excess vacancy concentration at a constant temperature as a function of hold time for vacancy decay mechanisms of different order: second order ($n = 2$)—red circles, first order ($n = 1$)—blue squares. (a) and (b) show, respectively, vacancy annihilation from an initial excess vacancy concentration 2 and 10 times higher than the equilibrium concentration. The horizontal, dashed line indicates half of the initial vacancy concentration. The downward pointing, colored arrows indicate the half-life of the relative excess vacancy concentration, which decreases with increasing excess vacancy concentration for $n = 2$ and remains constant for $n = 1$. The horizontal axes for both (a) and (b) are arbitrary but identical.

B. Estimated Material Parameters for Vacancy Annihilation as a Description of Conditioning

For a Pu-3.3 at.% Ga alloy, previous computational and experimental estimates suggest that $H_{vf} \approx 1$ eV.²⁸ If this value of H_{vf} is used as an approximation to a Pu-1.9 at.% Ga alloy, then one would estimate an equilibrium vacancy concentration of about 1.7×10^{-8} for plutonium held at 375 °C, the anneal temperature used in these experiments. If the annihilation of quenched-in vacancies is responsible for the conditioning effect in Pu-Ga, then the cooling rates used in the experiments must be capable of producing a significant amount of quenched-in vacancies. Furthermore, if the isothermal hold associated with conditioning represents the time-dependent annihilation of quenched-in vacancies, then the vacancy annihilation rate during conditioning should establish a time scale for conditioning, and that time scale should be compatible with experimental observations (*i.e.*, there should be significant vacancy annihilation in a matter of several hours, the timeframe over which conditioning occurs).

The caveat that vacancies be permitted to quench in upon cooling while still remaining sufficiently mobile at low temperature sets fairly restrictive conditions on the material-dependent constants of A and H_m . Increasing H_m means increasing the activation barrier for mov-

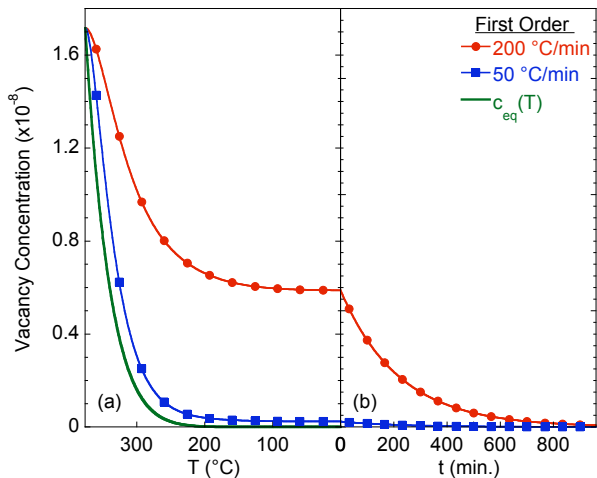


FIG. 4: Calculated vacancy concentration for first order vacancy annihilation as a function of both temperature during cooling from 375 °C to 0 °C (a) and subsequent isothermal hold time at 0 °C (b). Note that the temperature axis of (a) is reversed, with temperature decreasing to the right. Two different cooling rates are shown: $\nu = 200$ °C/min, red circles; and $\nu = 50$ °C/min, blue squares. As a reference, the equilibrium vacancy concentration is included as a solid green line. The vertical axis gives the concentrations in units of 10^{-8} . See text for the values of A and H_m

ing a vacancy, which tends to promote a higher concentration of quenched-in vacancies on cooling, but also tends to prohibit vacancy mobility at low temperature, as there is insufficient thermal energy to overcome the activation barrier. On the contrary, increasing A effectively increases the rate at which a vacancy annihilates, which tends to reduce or eliminate any quenched-in vacancies on cooling, but permits increased vacancy mobility to lower temperatures. There is thus a small window where the opposing tendencies of H_m and A produce an environment wherein the conditioning effect can be attributed to vacancy annihilation. The values of H_m and A can be adjusted slightly within this window, as there is currently no strict experimental criterion fixing the amount of excess vacancies after the quench, but large deviations from these values do not simultaneously satisfy the conditions of quenched-in vacancies after cooling and vacancy mobility at low temperature.

Figures 4 and 5 show calculated vacancy concentrations versus temperature and time for first and second order decay processes. Figures 4(a) and 5(a) exhibit the evolution of vacancy concentration upon cooling from 375 °C to 0 °C for two different experimental cooling rates. Figures 4(b) and 5(b) display the time-dependent decay of excess, quenched-in vacancies for isothermal holds at 0 °C following the quench from elevated temperature. Higher order vacancy annihilation processes are excluded for brevity. While it is clearly possible to choose values of A and H_m such that the experimental quench

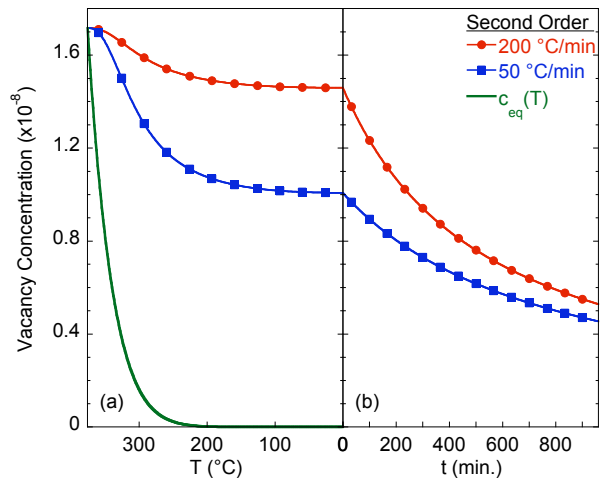


FIG. 5: Calculated vacancy concentration similar to that of Figure 4, but for second order vacancy annihilation. See text for the values of A and H_m

rates produce excess vacancies whose concentration can decay toward equilibrium at low temperature, the material parameters necessary to satisfy the aforementioned caveats should be examined further to understand their implications on the vacancy annihilation mechanisms.

For the case of a first order vacancy annihilation mechanism (Figure 4), $H_m \approx 0.25$ eV and $A \sim 10$ jumps/second. The value of H_m is about half of that proposed by Fluss *et al.*,²⁸ and significantly lower than typical values for other metals. While this estimate of H_m seems low in comparison to previous reports, the value of A seems unnaturally low. The constant A is proportional the jump frequency of a vacancy, typically of order 10^{12} - 10^{15} ,²⁹ and the number of jumps before a vacancy is annihilated. It is difficult to imagine a scenario where the jump frequency is low enough or the number of jumps before a vacancy annihilates is high enough to yield this low value of A . The values of A and H_m necessary to describe the conditioning of Pu-Ga alloys as a first order vacancy annihilation process seem unphysical, and likely exclude this scenario.

For a second order vacancy annihilation process, the case for compatibility with experimental observations is improved over that of a first order mechanism. To produce the curves of Figure 5, a value of $H_m \approx 0.2$ eV was used, similar to that used for the first order process, and, again, lower than previously reported by over 50%. The constant $A \sim 1 \times 10^7$ for the second order case, however, is six orders of magnitude greater than that of the first order case. While this value is still lower than what might be expected for conventional metals, it is more reasonable. This means that second order or higher vacancy annihilation mechanisms are not precluded as a description of conditioning simply by means of unphysical material constants, although the veracity of these constants—

which are still far from conventional—would need to be investigated via direct measurements of vacancy concentration.

C. Vacancy-derived Conditioning Compared with Experimental Results

The measured heats of reversion, shown above in Figure 2 as a function of conditioning time, is not a direct probe of the vacancy concentration. Instead, the measured heat of reversion is an indirect probe of the amount of martensitic transformation formed upon cooling:

$$\Delta H_a = f_a \Delta H^{\alpha' \rightarrow \delta},$$

where ΔH_a represents the measured heat of reversion—that is, the enthalpy change of the entire sample; f_a the fractional amount of martensitic transformation, itself dependent upon the details of any conditioning treatment; and $\Delta H^{\alpha' \rightarrow \delta}$ the heat of reversion for the $\alpha' \rightarrow \delta$ reversion, which is a constant value describing the phase change where a specific volume of the α' phase transforms entirely to the δ phase. While not a direct probe, the measured heat of reversion, being different from the fractional transformation only by a constant, can be used to illuminate the possibility of describing conditioning as vacancy annihilation. We start by assuming that conditioning can be described by the annihilation of excess quenched-in vacancies, and then compare the experimental results with the logical conclusions that must follow from that initial assumption.

1. If vacancy annihilation is the responsible mechanism for conditioning, then the first conclusion is that vacancy concentration must affect the amount of transformation, as it is known that conditioning increases the amount of transformation and, by proportionality, the heat of reversion. Unfortunately, there is no *a priori* or empirical knowledge regarding the specific functional dependence of the fractional amount of α' martensite formed with respect to vacancy concentration, but the measured fractional transformation can be generally expressed as:

$$f_a = f_{max} g(c),$$

where f_{max} is the maximum fractional amount of martensitic transformation and $g(c)$ is an unspecified function relating the fractional transformation to the vacancy concentration.

Equations 5 and 7 indicate that the concentration of vacancies at a constant temperature will decrease with time toward c_{eq} . From experiment, it is known that H_a increases with increasing hold time. These

two facts would imply that $g(c)$ should be bounded such that $0 \leq g(c) \leq 1$ with $g(c_{eq}) = 1$ and $g(c) \rightarrow 0$ as c increases (*i.e.*, longer conditioning times yield lower vacancy concentrations, which yield higher values of g , which yield higher fractional transformation). The time-dependent behaviors of both H_a and c are monotonic, so it would be natural to constrain $g(c)$ to be a monotonically decreasing function of vacancy concentration. Therefore, the measured heat can then be expressed as:

$$H_a = f_{max} \Delta H^{\alpha' \rightarrow \delta} g[c(t)], \quad (8)$$

where the time dependence of H_a and g arise intrinsically from the implicit time dependence of the vacancy concentration. The experimental data exhibit a gentle, s-shaped or sigmoid curve with time, but the time-dependent vacancy annihilation expressions of Equation 5 are of positive curvature everywhere, and do not exhibit any inflection. To comply with experiment, $g(c)$ is required to be a sigmoid function with an inflection point.

2. The experimental results above show that there is a conditioning effect for both the 50-°C/min and 200-°C/min quenches. If conditioning is described by vacancy annihilation, then it must be possible to trap quenched-in vacancies during the quench. Continuing, if vacancies can become quenched-in, then the concentration of quenched-in vacancies following the quench must be greater for the higher cooling rate, as described by Equations 5 and 6. Therefore, the initial vacancy concentration following the 200-°C/min quench must have resulted in a greater concentration of quenched-in vacancies than the 50-°C/min quench.
3. The next conclusion that can be deduced relates to vacancy annihilation from two different starting concentrations. From Equation 5, it can be derived that a larger initial concentration of vacancies results in a larger concentration after time t ; that is:

$$\frac{\partial(c - c_{eq})}{\partial(c_0 - c_{eq})} \geq 0$$

for all times. This effect can be observed in both Figures 4(b) and 5(b), where, for any time, the curves corresponding to the larger initial vacancy concentrations at $t = 0$ remain higher than those with the lower initial concentration of vacancies.

Therefore, following the 200-°C/min and 50-°C/min quenches, the vacancy concentration associated with the faster cooling rate should be greater for all times during the conditioning treatment. If c corresponding to the 200-°C/min quench is greater than that corresponding

to the 50-°C/min quench for all times, then $g(c)$ must be smaller for all times, implying that H_a for the 200-°C/min quench should be less than or equal to that of the 50-°C/min quench for all times. Qualitatively this conclusion is inconsistent with the data of Figure 2, where the faster quench rate yields a higher amount of transformation at low times. Since this conclusion does not adequately reproduce the qualitative evolution of the measured heat with increasing quench rate, then the initial assumption that vacancy annihilation is responsible for conditioning must be incorrect.

This conclusion can be further framed quantitatively if we choose a functional form for $g(c)$ satisfying the aforementioned criteria, arbitrarily choose an order for the vacancy annihilation mechanism, and fit the resultant form of Equation 8 to the experimental values of H_a . If we assume a first order vacancy annihilation mechanism and let $g(c) = \exp(-ac^p)$ ($p > 1$), then Equation 8 becomes

$$H_a(t) = C_1 \exp[-C_2 \exp(-C_3 t)], \quad (9)$$

where $C_1 = f_{max} \Delta H^{\alpha' \rightarrow \delta}$, which is independent of quench rate and serves as the asymptote to which any conditioning treatment, regardless of initial vacancy concentration, should converge; $C_2 = a(c_0 - c_{eq})$, for which the second term changes with quench rate while a is a constant; and $C_3 = rp$, which is also independent of quench rate.

Figure 6 displays the data from Figure 2 with fits to Equation 9 (solid lines), which can reasonably reproduce the important features of the data corresponding to the 50-°C/min quench if $C_1 \approx 925$ mJ/g, $C_2 \approx 23$, and $C_3 \approx 1.4$ hrs⁻¹. For the case of the 200-°C/min quench, the parameters C_1 and C_3 should be identical to the slower cooling rate, but C_2 is permitted to vary from the slower cooling rate by virtue of the initial concentration of quenched-in vacancies. In order to encompass the more rapid upturn of the measured heat, $C_2 \approx 7$ for the 200-°C/min quench. This resulting fit does not describe well the data for the faster quench rate; the fit saturates much earlier than the data suggest. Furthermore, as mentioned above, the faster quench should result in more quenched-in vacancies, which constrains C_2 for the 200-°C/min quench to be no less than that of the 50-°C/min quench. Thus, the best-fit value of C_2 in Figure 6 for the 200-°C/min quench is unphysical; it seems an unlikely possibility to describe simultaneously both the 50-°C/min and 200-°C/min quench data with classical vacancy annihilation.

V. CONCLUSIONS

While there are some features of the conditioning effect in Pu-Ga alloys that resemble the decay of excess,

quenched-in vacancies through annihilation, conditioning is not likely described by classical vacancy annihilation.

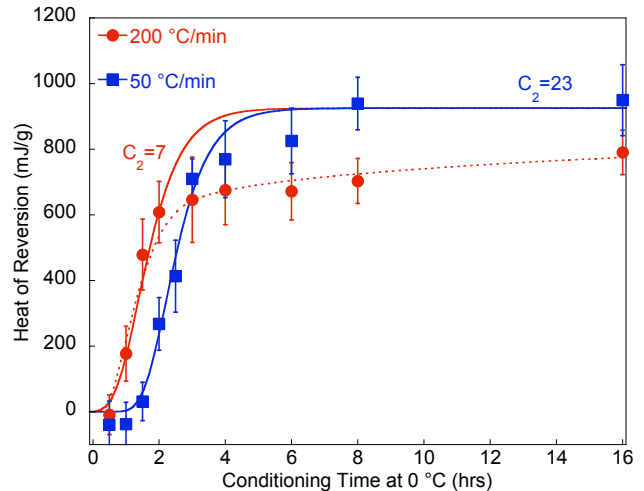


FIG. 6: Measured heat of reversion as a function of conditioning time with fits to Equation 9 (solid lines). Parameters can be chosen to provide a good fit to the 50-°C/min quench data, but the fit for the 200-°C/min quench is both unrepresentative of the data and unphysical (see text). The dotted line is a guide to the eye for the 200-°C/min quench data.

If vacancy annihilation is assumed as a description of conditioning, then the implications of that assumption do not agree well with the experimental findings. Estimates of the material constants that govern vacancy annihilation seem far from conventional, and the measured heat does not evolve as expected with increasing quench rate. It is clear that the quench rate from the anneal temperature to the conditioning temperature *does* have an effect upon the amount of transformation, but the mechanism by which the faster quench rate produces a more rapid rise in the amount of transformation is currently not understood. More work is necessary to propose a microscopic mechanism capable of describing conditioning in general, but that description should account for the dependence upon quench rates found here.

Acknowledgments

Lawrence Livermore National Laboratory is operated by Lawrence Livermore National Security, LLC, for the U.S. Department of Energy, National Nuclear Security Administration under Contract DE-AC52-07NA27344. This work was funded by the Laboratory Directed Research and Development Program at LLNL under project tracking code 07-ERD-047.

-
- ¹ See, for example, J. W. Christian, *The Theory of Transformation in Metals and Alloys* (Pergamon, Oxford, 2002).
- ² T. Kakeshita, K. Shimizu, S. Funada, and M. Date, *Acta Metall.* **33**, 1381 (1985).
- ³ V. A. Lobodyuk and E. I. Estrin, *Phys.-Usp.* **48**, 713 (2005).
- ⁴ A. Bag, K. K. Ray, and E. S. Dwarakadasa, *Metall. Mater. Trans. A* **30**, 1193 (1999).
- ⁵ A. Planes, F.-J. Pérez-Reche, E. Vives, L. Mañosa, *Scripta Mater.* **50**, 181 (2004).
- ⁶ L. Kaufman and M. Cohen, *Prog. Met. Phys.* **7**, 165 (1958).
- ⁷ J. T. Orme, M. E. Faiers, B. J. Ward, in *Plutonium 1975 and other Actinides*, edited by H. Blank and R. Lindner (North-Holland, Amsterdam, 1975).
- ⁸ S. S. Hecker, D. R. Harbur, and T. G. Zocco, *Prog. Mater. Sci.* **49**, 429 (2004).
- ⁹ S. S. Hecker, *Metall. Mater. Trans. A* **39A**, 1585 (2008).
- ¹⁰ K. T. Moore and G. van der Laan, *Rev. Mod. Phys.* **81**, 235 (2009).
- ¹¹ A. J. Schwartz, H. Cynn, K. J. M. Blobaum, M. A. Wall, K. T. Moore, W. J. Evans, D. L. Farber, J. R. Jeffries, and T. B. Massalski, *Prog. Mater. Sci.* (in press) (2009).
- ¹² S. S. Hecker, *Los Alamos Sci.* **26**, 290 (2000).
- ¹³ G. B. Olson and P. H. Adler, *Scripta Metall.* **18**, 401 (1984).
- ¹⁴ K. T. Moore, C. R. Krenn, M. A. Wall, and A. J. Schwartz, *Metall. Mater. Trans A* **38A**, 212 (2007).
- ¹⁵ J. R. Jeffries, K. J. M. Blobaum, M. A. Wall, and A. J. Schwartz, *Acta Mater.* **57**, 1831 (2009).
- ¹⁶ K. J. M. Blobaum, C. R. Krenn, M. A. Wall, T. B. Massalski, and A. J. Schwartz, *Acta Mater.* **54**, 4001 (2006).
- ¹⁷ T. Ohba, Y. Emura, and K. Otsuka, *Mater. Trans. JIM* **33**, 29 (1992).
- ¹⁸ M. Kozuma, Y. Murakami, T. Kawano, and K. Otsuka, *Scripta Mater.* **36**, 253 (1997).
- ¹⁹ Y. Murakami, Y. Nakajima, and K. Otsuka, *Scripta Mater.* **34**, 955 (1996).
- ²⁰ M. S. Wechsler, *Acta Metall. Mater.* **5**, 150 (1957).
- ²¹ Q. Wang, F. Han, J. Wang, and Q. Wang, *Phys. Stat. Sol. (a)* **202**, 72 (2005).
- ²² M. Stipcich and R. Romero, *Mater. Sci. Eng. A* **437**, 328 (2006).
- ²³ J. R. Jeffries, K. J. M. Blobaum, M. A. Wall, and A. J. Schwartz, *J. Nucl. Mater.* **384**, 222 (2009).
- ²⁴ K. J. M. Blobaum, C. R. Krenn, J. N. Mitchell, J. J. Haslam, M. A. Wall, T. B. Massalski, and A. J. Schwartz, *Metall. Mater. Trans. A* **37A**, 567 (2006).
- ²⁵ See, for example, R. E. Reed-Hill, *Principles of Physical Metallurgy*, 3rd edition (PWS Publishing Company, Boston, MA, 1994).
- ²⁶ A. Schulze and K. Lücke, *Acta Metall.* **20**, 529 (1972).
- ²⁷ A. B. Ziya, M. I. Ansari, and A. A. Al-Aql, *J. Alloy. Compd.* **337**, 108 (2002).
- ²⁸ M. J. Fluss, B. D. Wirth, M. Wall, T. E. Felter, M. J. Caturla, A. Kubota, and T. Diaz de la Rubia, *J. Alloy. Compd.* **368**, 62 (2004).
- ²⁹ W. Schüle and A. Panzarasa, *J. Phys F: Metal Phys.* **10**, 1375 (1980).